Rice zinc finger protein DST enhances grain production through controlling *Gn1a/OsCKX2* expression

Shuyu Li[a,1], Bingran Zhao[b,1], Dingyang Yuan[b,1], Meijuan Duan[b,1], Qian Qian[c,1], Li Tang[b], Bao Wang[a], Xiaoqiang Liu[a], Jie Zhang[a], Jun Wang[a], Jiaqiang Sun[a], Zhao Liu[d], Yu-Qi Feng[d], Longping Yuan[b,2], and Chuanyou Li[a,2]

[a]State Key Laboratory of Plant Genomics, National Center for Plant Gene Research, Institute of Genetics and Developmental Biology, Chinese Academy of Sciences, Beijing 100101, China; [b]State Key Laboratory of Hybrid Rice, China National Hybrid Rice Research and Development Center, Changsha 410125, China; [c]State Key Laboratory of Rice Biology, China National Rice Research Institute, Chinese Academy of Agricultural Sciences, Hangzhou 310006, China; and [d]Key Laboratory of Analytical Chemistry for Biology and Medicine (Ministry of Education), Department of Chemistry, Wuhan University, Wuhan 430072, China

Contributed by Longping Yuan, January 8, 2013 (sent for review December 5, 2012)

The phytohormone cytokinin (CK) positively regulates the activity and function of the shoot apical meristem (SAM), which is a major parameter determining seed production. The rice (*Oryza sativa* L.) *Gn1a*/*OsCKX2* (*Grain number 1a*/*Cytokinin oxidase 2*) gene, which encodes a cytokinin oxidase, has been identified as a major quantitative trait locus contributing to grain number improvement in rice breeding practice. However, the molecular mechanism of how the expression of *OsCKX2* is regulated in planta remains elusive. Here, we report that the zinc finger transcription factor DROUGHT AND SALT TOLERANCE (DST) directly regulates *OsCKX2* expression in the reproductive meristem. DST-directed expression of *OsCKX2* regulates CK accumulation in the SAM and, therefore, controls the number of the reproductive organs. We identify that *DST*^{reg1}, a semidominant allele of the *DST* gene, perturbs DST-directed regulation of *OsCKX2* expression and elevates CK levels in the reproductive SAM, leading to increased meristem activity, enhanced panicle branching, and a consequent increase of grain number. Importantly, the *DST*^{reg1} allele provides an approach to pyramid the *Gn1a*-dependent and *Gn1a*-independent effects on grain production. Our study reveals that, as a unique regulator of reproductive meristem activity, DST may be explored to facilitate the genetic enhancement of grain production in rice and other small grain cereals.

transcriptional regulation | cytokinin metabolism | inflorescence meristem

As one of the most important staple food crops, rice (*Oryza sativa* L.) is cultivated worldwide and feeds more than one-half of the world's population. Accordingly, enhanced grain yield is a major focus of rice breeding programs worldwide (1, 2). Rice grain yield is mainly determined by three components, including number of panicles per plant, grain number per panicle, and grain weight. Among them, grain number per panicle is highly variable and contributes to the most part of grain yield formation (1, 3). During the panicle development stage, the inflorescence meristem, which produces flowers that form seeds after fertilization, is a central determinant of grain number formation. Recently, many studies in rice reveal that a reduction in meristem activity leads to reduced panicle branching and grain production (4–6). By contrast, several high yield genes known as quantitative trait loci (QTLs) in rice show an enhancing effect on meristem activity, panicle branching, and grain production (7–14). Therefore, the size and activity of the reproductive meristem is a crucial parameter determining grain production of rice.

Among the known factors controlling shoot apical meristem (SAM) activity are transcriptional regulators and the plant hormone cytokinin (CK) (15, 16). Experimental reduction of the CK status, either by lowering the CK levels or by reducing CK signaling, abbreviates the SAM activity (17–22). On the contrary, an elevated CK level is associated with increased SAM activity (23, 24). It was shown that the rice *Gn1a* (*Grain number 1a*) locus, a major QTL for increasing grain number, harbors a mutation in the *OsCKX2* gene, which encodes a CK oxidase/dehydrogenase (CKX) that catalyzes the degradation of active CKs (7). Reduced expression of *OsCKX2* causes CK accumulation in inflorescence meristems and increases the number of reproductive organs, which results in enhanced grain production (7). Prominently, mutation alleles of *OsCKX2* have been successfully used in rice breeding practice to improve seed production (7). The relationship between *CKX* genes and seed production also exists in the dicotyledonous model plant *Arabidopsis thaliana*. It was shown recently that simultaneous mutation of *CKX3* and *CKX5* of *Arabidopsis* elevates CK levels and, thereby, leads to increased SAM activity and seed yield (25).

Although the importance of *CKX* genes in SAM maintenance and seed production are well recognized in both monocots and dicots, the regulatory mechanisms governing the expression of these CK metabolic genes remain elusive (26). To identify molecular components controlling *OsCKX2* expression, we set up a genetic screen and identified a unique rice mutant, *regulator of Gn1a 1* (*reg1*), which shows reduced *OsCKX2* expression, elevated meristem activity, and increased grain number. Here, we report that the *reg1* phenotype was caused by a semidominant mutation of the *DST* (*DROUGHT AND SALT TOLERANCE*) gene, which encodes a zinc finger protein that regulates drought and salt tolerance in rice (27). Molecular evidence shows that the DST transcription factor regulates the reproductive SAM activity through controlling the expression of *OsCKX2*. We found that the *DST*^{reg1} allele perturbs DST-directed regulation of *OsCKX2* expression and elevates CK levels in the inflorescence meristem, leading to increased SAM activity and a consequent increase of grain production. Importantly, the *DST*^{reg1} allele provides a breeding tool to pyramid the *Gn1a*-dependent and *Gn1a*-independent effects on grain production of rice.

Results

***reg1* Mutant Shows Elevated SAM Activity and Enhanced Grain Production.** To gain more insight into the genetic networks controlling SAM activity and grain production, we identified and characterized a rice mutant, *reg1*. Compared with its wild-type Zhefu 802 (ZF802), a cultivated *indica* rice variety in China, the *reg1* mutant showed increased plant stature (Fig. 1*A*) and enlarged panicle size (Fig. 1*B*). Close examination revealed that the SAM of *reg1* was larger than that of ZF802 (Fig. 1 *C* and *E*), suggesting an enhancing effect of *reg1* on SAM activity. In comparison with ZF802, the *reg1* panicle produced more primary (Fig.

Author contributions: S.L., L.Y., and C.L. designed research; S.L., B.Z., D.Y., M.D., Q.Q., L.T., B.W., X.L., J.Z., J.W., J.S., Z.L., and Y.-Q.F. performed research; S.L., L.Y., and C.L. analyzed data; and S.L., L.Y., and C.L. wrote the paper.

The authors declare no conflict of interest.

Freely available online through the PNAS open access option.

[1]S.L., B.Z., D.Y., M.D., and Q.Q. contributed equally to this work.

[2]To whom correspondence may be addressed. E-mail: cyli@genetics.ac.cn or lpyuan@hhrrc.ac.cn.

This article contains supporting information online at www.pnas.org/lookup/suppl/doi:10.1073/pnas.1300359110/-/DCSupplemental.

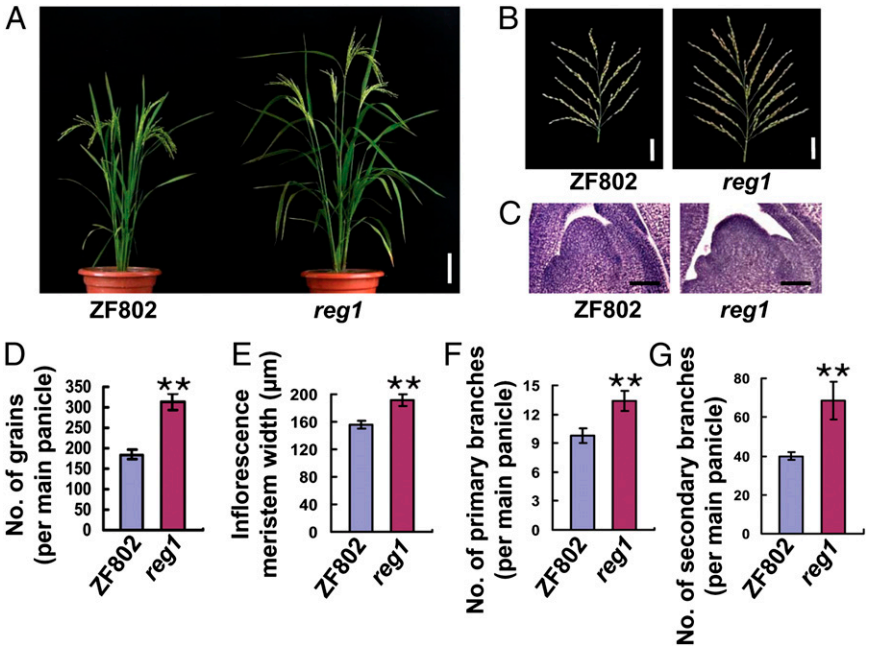

Fig. 1. Morphological comparison between wild-type and the *reg1* mutant. (*A*) Gross morphologies of ZF802 and *reg1*. (*B*) The panicle morphologies of ZF802 and *reg1*. (*C*) Longitudinal sections of the inflorescence meristem of ZF802 and *reg1*. (Scale bars: *A*, 20 cm; *B*, 5 cm; *C*, 50 μm.) (*D*) Comparison of grain number per main panicle between ZF802 and *reg1*. (*E*) Comparison of inflorescence meristem width between ZF802 and *reg1*. (*F*) Comparison of primary branch number per main panicle between ZF802 and *reg1*. (*G*) Comparison of secondary branch number per main panicle between ZF802 and *reg1*. Samples in *C* and *E* are inflorescence meristem just after the phase change from vegetative to reproductive stage. Values in *D*–*G* are means with SD ($n = 30$ plants). The double asterisks represent significant difference determined by the Student *t* test at $P < 0.01$.

1*F*) and secondary branches (Fig. 1*G*) and, eventually, led to an increase of grain number per main panicle by 63.8% (Fig. 1*D*). To evaluate the effect of *reg1* on grain production in field conditions, we performed yield test assay. The *reg1* mutation increased grain yield by 31.2% over ZF802 in the test plot (Table 1). Statistical analysis of the three major components of grain yield indicated that, compared with ZF802, the *reg1* mutation actually reduced panicle number by 23.7%, but increased 1,000-grain weight by 9.9% and grain number per panicle by 56.5% (Table 1). These data support that the *reg1* mutation defines a grain number enhancing gene whose function is tightly associated with SAM activity.

Cloning and Characterization of *REG1*. Genetic analysis indicated that *reg1* was a semidominant mutant, given that the phenotypes of heterozygous plants were intermediate between those of the homozygous *reg1* plants and their wild-type counterparts (Fig. S1). Fine mapping using 2,020 mutant F_2 plants delimited the *REG1* locus to a 19-kb region on chromosome 3, in which only one gene, named *LOC_Os03g57240*/*DST*, is predicted (Fig. 2 *A* and *B*). DNA sequencing revealed that *reg1* contains an A insertion between the 214th and 215th nucleotides of the *DST* cDNA (cDNA) (Fig. 2*C*). It was recently shown that *DST* encodes a zinc finger protein that negatively regulates drought and salt tolerance of rice plants (27).

To confirm that mutation of *DST* underlies the *reg1* phenotype, we generated transgenic plants expressing different levels of *DST* in Nipponbare (NP), a *japonica* variety suitable for transformation. All transgenic plants overexpressing a wild-type *DST* allele (DST^{REG1}) showed reduced plant stature with less panicle branches and decreased grain number (Fig. S2 *A*–*D*). In contrast, the *DST* RNA interference (RNAi) transgenic plants showed increased panicle branches and enhanced grain number (Fig. S2 *E*–*H*). Similarly, transgenic plants overexpressing the *reg1* mutant allele of *DST* (DST^{reg1}) had increased panicle branches and produced more grains (Fig. S2 *I*–*L*). Therefore, the identified A insertion in the *DST* gene is responsible for the phenotype of the *reg1* mutation and that DST^{reg1} acts as a dominant negative regulator of reproductive meristem activity and grain production.

***reg1* Mutation Elevates CK Levels in the Meristem Through Reducing *OsCKX2* Expression.** Consistent with its effect on panicle branching and grain number formation, *DST* mRNA was richly expressed in the SAM, the primordia of primary branches, secondary branches, and young spikelets of developing panicles (Fig. 3 *A*–*E*). Considering that CKs play a positive role in regulating SAM activity and grain production, we examined the CK status in the SAM of *reg1*. RNA in situ hybridization showed that the transcript levels of *RESPONSE REGULATOR1* (*OsRR1*), a marker gene for CK response in the SAM (28, 29), were greatly increased in *reg1* than those in ZF802 (Fig. 3 *F*–*I*). Comparison of CK levels in the inflorescence meristem revealed that the contents of iP, iPR, and iP9G were substantially more abundant in *reg1* than those in ZF802 (Fig. 3*T*). To explore how *reg1* affects CK levels in the SAM, we examined the expression of *OsCKX2*, which has been shown to be important for SAM activity and seed production (7). RNA in situ hybridization revealed that, during different stages of inflorescence development, the expression levels of *OsCKX2* are

Table 1. Yield test in a paddy

Traits	ZF802	*reg1*	NIL 93–11-DST^{REG1}	NIL 93–11-DST^{reg1}	NIL NP-DST^{REG1}	NIL NP-DST^{reg1}
Panicles per plot	2,220.7 ± 46.2	1,695.3 ± 20.3	2,347.8 ± 36.2	2,049.2 ± 40.5	3,228.8 ± 58.4	2,539.2 ± 44.7
Grains per panicle	121.7 ± 1.3	190.5 ± 1.6	152.8 ± 2.3	208.5 ± 5.8	82.5 ± 2.3	122.6 ± 5.8
1,000-grain weight, g	24.3 ± 0.5	26.7 ± 0.5	30.8 ± 0.9	31.5 ± 0.8	20.1 ± 0.8	21.1 ± 0.8
Theoretical yield per plot, kg	6.6 ± 0.4	8.6 ± 0.3	11.0 ± 0.6	13.5 ± 0.3	5.4 ± 0.5	6.6 ± 0.7
Actual yield per plot, kg	5.4 ± 0.3	7.1 ± 0.2	8.8 ± 0.7	10.7 ± 0.7	4.4 ± 0.4	5.3 ± 0.7

Data are from plants in randomized complete block design with three replications under natural condition in Beijing, China, in 2011. The planting density was 25 cm × 25 cm, with one plant per hill. The area per plot was 13.34 m^2. Values are means with SD of three replications.

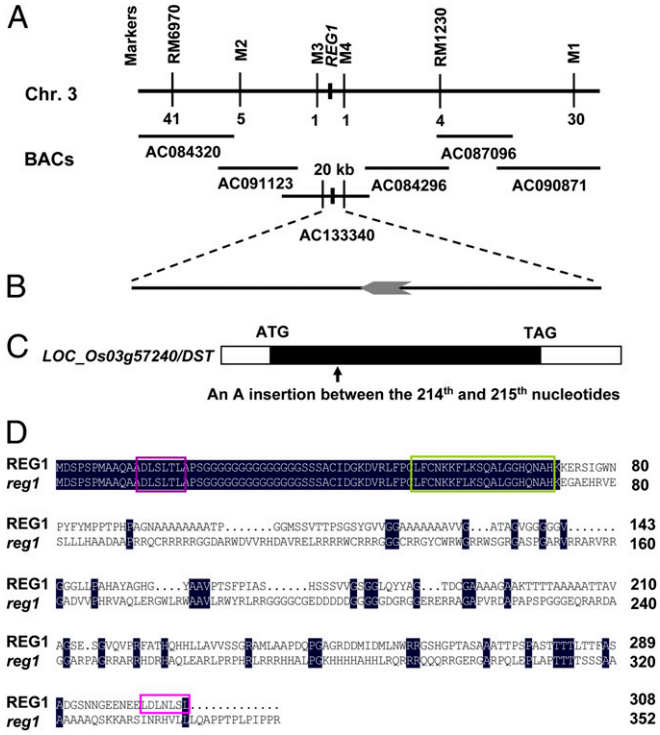

Fig. 2. Map-based cloning of *REG1*. (*A*) The *REG1* locus was mapped to an interval between the molecular markers RM6970 and M1 on chromosome 3. (*B*) Positional cloning narrowed the *REG1* locus to a 19-kb region between M3 and M4 at BAC AC133340. Only one gene is predicted in this region by the Rice Annotation Project Database. Numbers on the map indicate the number of recombinants. (*C*) The *REG1* structure and the mutation site in *reg1*. Predicted ORF and sequence differences between ZF802 and *reg1* at the *REG1* candidate region are shown. (*D*) Sequence alignment of the REG1 protein from ZF802 and the *reg1* mutant. Identical residues are indicated by dark gray boxes. The EAR motifs in the N-terminal and C-terminal are indicated by purple and pink frames, and the zinc finger domain is indicated by a green frame.

generally lower in *reg1* than those in ZF802 (Fig. 3 *J*–*Q*). Consistently, quantitative real-time PCR (qRT-PCR) assays indicated that the expression levels of *OsCKX2* (Fig. 3*R*) and several other members of the *OsCKX* family, including *OsCKX1*, *3*, *4*, *5*, and *9*, were considerably reduced in *reg1* than those in ZF802 (Fig. 3*S*). In addition, the expression levels of three cytokinin-*O*-glucosyltransferase genes including *LOC_Os02g51910*, *LOC_Os02g51930*, and *LOC_Os04g25440* are also reduced in *reg1*, which may contribute to the increased iP9G levels in the mutant (Fig. S3). These data support that DST^{reg1} reduces *OsCKX2* expression, elevates CK levels in the inflorescence meristem, and therefore increases seed production.

DST Directly Activates *OsCKX2* Expression. DST^{REG1} contains a highly conserved C2H2-type zinc finger domain and shows transcriptional activation activity (27). Notably, our sequence analysis identified that DST^{REG1} contains two ethylene-responsive element binding factor-associated amphiphilic repression (EAR) motifs (30–33), which located at the N-terminal and C-terminal of the DST^{REG1} protein (Fig. 2*D*). The EAR motif, which contains two distinct sequence conservation patterns—LxLxL and DLNxxP—is generally believed to be involved in negative or positive regulation of gene transcription (8, 9, 27, 32, 34–37). In the *reg1* mutant, the A insertion leads to a frameshift after the first 72 amino acids (Fig. 2*D*), which destroys the C-terminal EAR motif.

A yeast assay was performed to determine the transcriptional activation activity of DST^{REG1} and DST^{reg1}. As expected, DST^{REG1} exhibits transcription activation activity in the yeast assays, whereas DST^{reg1} does not (Fig. 4*A*), indicating that the *reg1* mutation abolishes the transcriptional activation capacity of the DST^{REG1} protein. Next, a series of protein truncations were generated to determine the domains required for the transcriptional activity of DST^{REG1}. Deletion of the N-terminal EAR did not affect

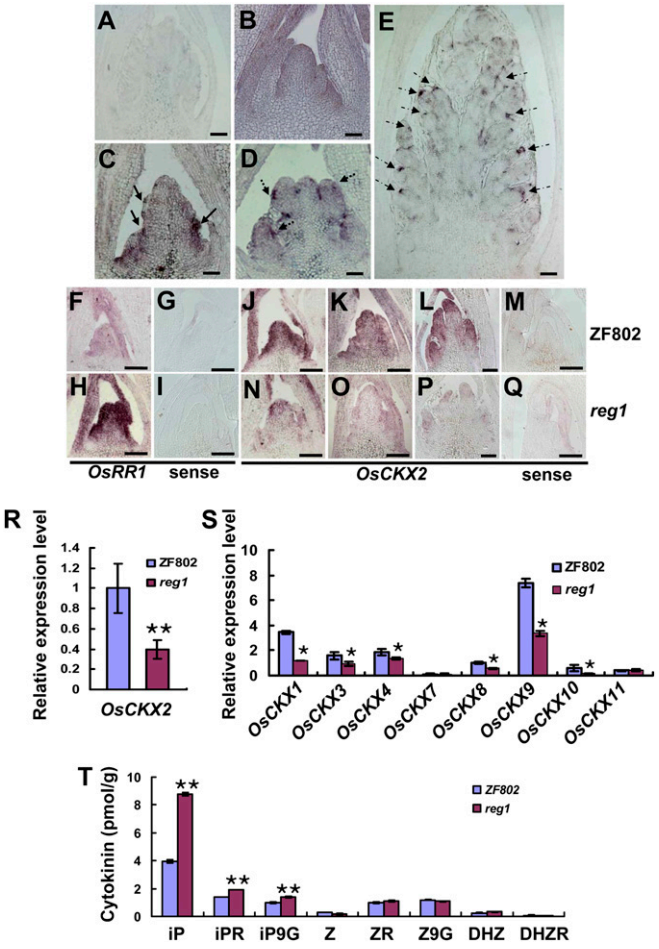

Fig. 3. The function of *reg1* mutation in the inflorescence meristem. (*A*–*E*) *DST* expression during panicle development revealed by RNA in situ hybridization. *A* is a negative control preparation made with a sense *DST* probe. *B* is just after the phase change from vegetative to reproductive stage. *C* is at the stage of primary branch meristem differentiation. *D* is at the stage of formation of primary branch primordia. *E* is at the stage of initiation of spikelet primordia. Arrows in *C*–*E* indicate primary branch primordia, secondary branch primodia, and floret primodia, respectively. (*F*–*I*) Expression of *OsRR1* in inflorescence meristems of ZF802 (*F* and *G*) and *reg1* (*H* and *I*) revealed by RNA in situ hybridization. Samples are inflorescence meristems just after the phase change from vegetative to reproductive stage. *F* and *H* are hybridization of *OsRR1*. *G* and *I* are hybridization of sense probes. (*J*–*Q*) Expression of *OsCKX2* in developing panicles of ZF802 (*J*–*M*) and *reg1* (*N*–*Q*) revealed by RNA in situ hybridization. *J* and *N* are just after the phase change from vegetative to reproductive stage. *K* and *O* are at the stage of primary branch meristem differentiation. *L* and *P* are at the stage of formation of primary branch primordia. *M* and *Q* are hybridization of sense probes. (Scale bars: 50 μm). (*R*) Transcript levels of *OsCKX2* in the inflorescence meristems of ZF802 and *reg1* revealed by qRT-PCR. Transcript levels of *OsCKX2* in ZF802 were arbitrarily set to 1. (*S*) Transcript levels of *OsCKXs* in the inflorescence meristems of ZF802 and *reg1* revealed by qRT-PCR. Transcript levels of *OsCKX8* in ZF802 were arbitrarily set to 1. (*T*) Comparison of CK levels in the inflorescence meristems of ZF802 and *reg1*. iP, isopentenyladenine; iPR, iP riboside; iP9G, iP 9-glucoside; Z, zeatin; ZR, zeatin riboside; Z9G, zeatin 9-glucoside. Values are means with SD ($n = 3$ measurements) in *R*–*T*. The asterisks in *R*–*T* represent significance difference determined by the Student *t* test at $P < 0.01$.

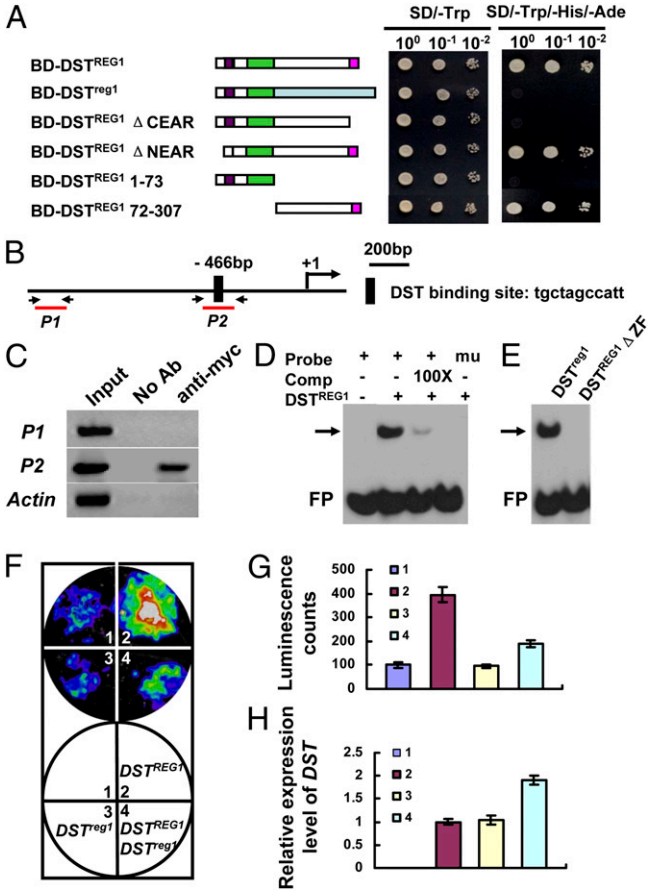

Fig. 4. DST^{REG1} promotes the expression of *OsCKX2*. (*A*) Transactivation activity assay in the yeast. BD, GAL4-DNA binding domain; DST^{REG1}, DST from ZF802; DST^{reg1}, DST from *reg1*. Purple box indicates N-terminal EAR motif; green box indicates zinc finger domain; and pink box indicates C-terminal EAR motif. (*B*) Schematic diagram of the promoter region of *OsCKX2*. Black box represents DST binding site. Numbers above indicate the distance away from the ATG. Region between the two coupled arrow indicates the DNA fragment used for ChIP-PCR. (*C*) ChIP assay shows the association of DST^{REG1} with the promoter of *OsCKX2*. Immunoprecipitation was performed with or without myc antibody (no Ab). (*D*) EMSA assay shows the binding of DST^{REG1} to the promoter of *OsCKX2*. (*E*) EMSA assay shows the binding of *pOsCKX2* with DST^{reg1} or DST^{REG1}ΔZF. In *D* and *E*, the arrows indicate the up-shifted bands; FP indicates free probe. (*F*) DST^{REG1} promotes *OsCKX2* expression in vivo. Tobacco leaves were transformed with *pOsCKX2:LUC* plus vector control (1), *pUBI:DST^{REG1}* (2), *pUBI:DST^{reg1}* (3), or *pUBI:DST^{REG1}* and *pUBI:DST^{reg1}* (4). (*G*) Statistics of luciferase activity in *F*. These experiments were repeated three times with similar results. (*H*) qRT-PCR analysis of the expression level of *DST* in *F*. Values in *G* and *H* are means with SD of three replicates.

transcription activation, whereas deletion of the C-terminal EAR abolished transcription activation activity (Fig. 4*A*), indicating that the C-terminal EAR, but not the N-terminal EAR, is required for the transcriptional activation of DST^{REG1} in the yeast system.

It has been shown that DST binds to the TGNTANN(A/T)T sequence, a *cis* element named DST-binding sequence (DBS) (27). Sequence analysis revealed the presence of DBS in the promoter regions of *OsCKX2* (Fig. 4*B*) and other *OsCKX* genes (Fig. S4). Chromatin immunoprecipitation assays using *35Spro:DST^{REG1}-4myc* transgenic plants and anti-myc antibodies indicated that DST was enriched in the *OsCKX2* promoter region containing the DBS (Fig. 4*C*). We then conducted DNA electrophoretic mobility shift assays (EMSA) to test that DST directly binds the DBS in vitro. For these experiments, full-length DST^{REG1} was expressed as a His-tag fusion protein in *Escherichia coli* and affinity purified. As shown in Fig. 4*D*, the DST^{REG1}-His fusion protein was able to bind DNA probes containing the DBS motif but failed to bind DNA probes containing a mutant form of the DBS. The addition of unlabeled DNA probes competed for the binding of DST^{REG1} to the DBS probes. Significantly, EMSA showed that DST^{reg1}, the mutant version of the DST protein, still can bind the DBS DNA probes; in contrast, DST^{REG1}ΔZF, in which the zinc finger domain of DST^{REG1} was deleted, lost this binding ability (Fig. 4*E*). Together, these data support that the *reg1* mutation does not affect the binding ability of the DST^{REG1} protein to the DBS motif in the promoter of *OsCKX2*.

Using the well-established transient expression assay of *Nicotiana benthamiana* leaves (38–40), we seek to determine the effect of DST^{REG1} and DST^{reg1} on the expression of a reporter containing the *OsCKX2* promoter fused with the firefly luciferase gene (*LUC*). When the *pOsCKX2:LUC* reporter was infiltrated into *N. benthamiana*, a substantial amount of LUC activity could be detected, indicating that endogenous factors of *N. benthamiana* may activate the expression of the *pOsCKX2:LUC* reporter. Coexpression of the *pOsCKX2:LUC* reporter with *DST^{REG1}* led to an obvious increase of the luminescence intensity (Fig. 4 *F–H*), indicating that DST^{REG1} activated the expression of *pOsCKX2:LUC*. In contrast, DST^{reg1} failed to increase the expression of *pOsCKX2:LUC* (Fig. 4 *F–H*), indicating that DST^{reg1} lost the ability to activate *pOsCKX2:LUC* expression, albeit this allele still can bind the *OsCKX2* promoter as revealed by EMSA assays (Fig. 4*E*). Importantly, coexpression of *DST^{reg1}* with *DST^{REG1}* substantially reduced the effect of *DST^{REG1}* on the activation of *pOsCKX2:LUC* expression (Fig. 4 *F–H*), providing another line of evidence that *DST^{reg1}* may compete *DST^{REG1}* for binding the promoter of the *pOsCKX2:LUC* reporter.

The above-described results support a scenario that, in *reg1* plants, the DST^{reg1} protein still can bind the *OsCKX2* promoter as DST^{REG1} does, but this mutant protein loses the transcriptional activation activity to promote *OsCKX2* expression. Competition between DST^{reg1} and DST^{REG1} could underlie that the *reg1* mutant shows a semidominant phenotype.

***DST^{reg1}* Enhances Grain Production in both *indica* and *japonic* Rice.** Because mutation alleles of *OsCKX2* have been successfully applied in rice breeding practice (7), our elucidation of the DST function to regulate *OsCKX2* expression highlights the feasibility to apply the *DST^{reg1}* allele in rice breeding to improve grain production. Like the reported variety 5150 (7), the high-yielding *indica* variety R498 contains an 11-bp deletion in the third exon of *OsCKX2* (Fig. S5*A*) and, therefore, impairs the expression of this CK catabolic gene (Fig. S5*C*). We developed a near isogenic line (NIL) in the genetic background of R498 that contains the *DST^{reg1}* allele. Consistent with a scenario that DST-mediated regulation of *OsCKX2* expression is involved in seed production, the resulting NIL R498-*DST^{reg1}* plants showed similar panicle size and grain number per panicle as NIL R498-*DST^{REG1}* did (Fig. 5 *A* and *B* and Fig. S6*A*).

In contrast to 5150 and R498, 93-11, another high-yielding *indica* variety from China (41), does not contain any mutation in *OsCKX2* (Fig. S5 *B* and *C*), suggesting that the high-yielding trait of 93-11 is contributed by QTLs other than *Gn1a*. To evaluate whether the *reg1* mutation can further enhance the seed production of this high-yielding *indica* rice, we generated NIL in the genetic background of 93-11 that contains the *DST^{reg1}* allele. The resulting NIL 93-11-*DST^{reg1}* showed increased primary and secondary panicle branching and produced more grains than its recurrent parent, NIL 93-11-*DST^{REG1}* (Fig. 5 *C* and *D* and Fig. S6*B*). In the yield test assay of field conditions, the NIL 93-11-*DST^{reg1}* increased grain yield by 21.6% over NIL 93-11-*DST^{REG1}* (Table 1).

To evaluate the effect of the *reg1* mutation on yield enhancement in *japonica* rice, we generated *DST^{reg1}* NIL in the genetic background of NP, which does not contain any mutation in the

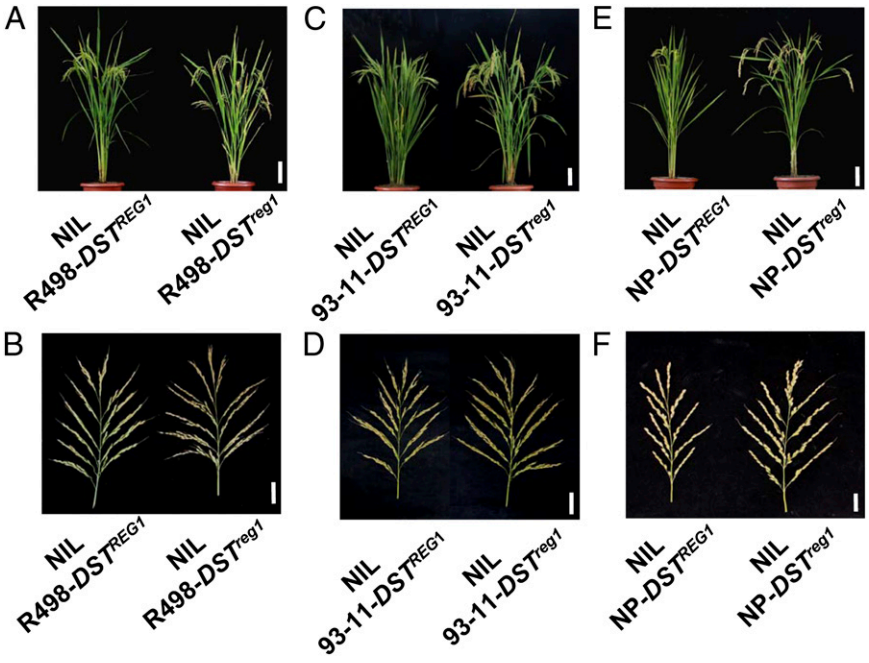

Fig. 5. Effect of the *DST*^{reg1} mutation on grain number formation in different alleles of *Gn1a*/*OsCKX2*. (*A*) Gross morphologies of NIL R498-*DST*^{REG1} and NIL R498-*DST*^{reg1} at the mature stage. (*B*) Comparison of the panicle morphologies of NIL R498-*DST*^{REG1} and NIL R498-*DST*^{reg1}. (*C*) Gross morphologies of NIL 93-11-*DST*^{REG1} and NIL 93-11-*DST*^{reg1} at the mature stage. (*D*) Comparison of the panicle morphologies of NIL 93-11-*DST*^{REG1} and NIL 93-11-*DST*^{reg1}. (*E*) Gross morphologies of NIL NP-*DST*^{REG1} and NIL NP-*DST*^{reg1} at the mature stage. (*F*) Comparison of the panicle morphologies of NIL NP-*DST*^{REG1} and NIL NP-*DST*^{reg1}. (Scale bars: *A*, *C*, and *E*, 20 cm; *B*, *D*, and *F*, 5 cm.)

OsCKX2 locus (Fig. S5 *B* and *C*). As expected, NIL NP-*DST*^{reg1} showed increased panicle branching and produced more grains per panicle in comparison with NIL NP-*DST*^{REG1} (Fig. 5 *E* and *F* and Fig. S6*C*). In the yield test assay of field conditions, the NIL NP-*DST*^{reg1} increased grain yield by 20.5% over NIL NP-*DST*^{REG1} in the test plot (Table 1). Taken together, our results indicate that the *reg1* allele of the *DST* gene is applicable to pyramid the *Gn1a*-dependent and *Gn1a*-independent yield enhancing effects in both *indica* and *japanic* rice.

***DST*^{reg1} Enhances Grain Number in Wheat.** Sequence analysis identified DST homologs in small grain cereals including barley and wheat (Fig. S7*A*), suggesting functional conservation of this protein. To investigate the possible effect of DST on grain production in wheat, we generated a number of transgenic wheat plants carrying *DST*^{REG1} and *DST*^{reg1}. Transgenic wheat lines with increased expression of *DST*^{REG1} show a decrease in the length of the ear and a reduced number of spikelets, whereas transgenic wheat lines with increased expression of *DST*^{reg1} showed increased ear size and spikelet number (Fig. S7 *B* and *C*). These data suggest an application potential of *DST*^{reg1} in wheat breeding to increase grain yield.

Discussion

The bioactive CK status of the SAM is determined by many factors, including the biosynthesis, activation, and degradation of the hormone. Accumulating evidence indicated that the action of CK in maintaining SAM activity is tightly linked to transcription factors involved in the activation or repression of the expression of CK-related genes (16, 42). For example, the Class I KNOTTED1-like homeobox (KNOXI) proteins, which are essential for SAM maintenance and function, act in part through regulating the expression of *ISOPENTENYL TRANSFERASE7* (*IPT7*), which encodes a rate-limiting enzyme for CK biosynthesis (43–45). Although the role of the *CKX* genes in maintaining SAM function and seed production is well recognized in both monocots and dicots, less is known about how the expression of these genes is regulated in planta (7, 25, 26). We report here that the rice *Gn1a*/*OsCKX2* gene, which has been used as a breeding tool, is under the direct regulation of the zinc finger transcription factor DST^{REG1}. Several lines of evidence support this finding. First, DST^{REG1} is a transcription activator and its C-termial EAR motif is required for its transcriptional activity. Second, as revealed by EMSA and ChIP assays, DST^{REG1} specifically binds to the DBS motif in the promoter of *OsCKX2*. Third, transactivation assays in *N. benthamiana* leaves support that DST^{REG1} stimulates the activity of LUC as a reporter driven by *OsCKX2* promoter. Given that both DST^{REG1} (this work) and OsCKX2 (7) are important for the SAM function and seed production, our results reveal a unique pathway in which a transcription factor directly links to a specific CK metabolic gene in the regulation of the SAM function. Indeed, we show that DST-executed expression of *OsCKX2* contributes to the accumulation of CKs in the SAM and, therefore, plays a crucial role in SAM maintenance. In the *reg1* mutant, the DST^{reg1} still binds the DBS motif of the *OsCKX2* promoter, but losses the ability to activate the expression of *OsCKX2*; reduced expression of *OsCKX2* leads to increased CK accumulation in the SAM, which renders enhanced seed production of *reg1*.

Significantly, our finding provides a strategy to apply the *DST*^{reg1} allele in rice breeding practice. Because total grain number per plant is the most important factor for increasing grain yield under field production conditions, rice breeders have been devoted to identifying QTLs showing enhanced effect on grain number (7–14). Among them, *Gnla*/*OsCKX2* has been molecularly characterized and successfully applied in rice breeding (7). Pyramiding the grain number enhancing effects of Gn1a (i.e., Gn1a-dependent) and other QTLs (i.e., Gn1a-independent) is a major target of rice breeding program (7). We provide evidence showing that, when the *DST*^{reg1} allele is introduced into rice varieties that do not contain a *Gn1a* mutation, the resulting NILs show substantial grain number enhancing effect. Therefore, *DST*^{reg1} is applicable in conventional rice breeding program to pyramid the *Gn1a*-dependent and *Gn1a*-independent QTLs for grain production. Importantly, the semidominant nature of *DST*^{reg1} renders that this mutation allele is especially suitable for hybrid rice breeding. In addition, ectopic expression of *DST*^{reg1} in wheat leads to increased grain production, suggesting an application potential of DST or its homologs in other small grain cereals.

Intriguingly, the zinc finger transcription factor DST was also shown to regulate drought and salt tolerance via stomatal control (27). In this case, the zinc finger motif of DST is required for its transactivation activity to regulate genes involved in the homeostasis

of reactive oxygen species. Loss of DST function increases stomatal closure and reduces stomatal density, consequently resulting in enhanced drought and salt tolerance in rice (27). This observation, together with our finding that DST contributes to seed production via controlling CK degradation, indicate that DST plays a dual role in regulating development and stress response.

Materials and Methods

Cytokinin Analysis. Extraction and determination of CKs from rice young panicles (<0.5 cm) were performed by using a polymer monolith microextraction/hydrophilic interaction chromatography/electrospray ionization-tandem mass spectrometry method as described (46).

RNA in Situ Hybridization. RNA in situ hybridization was performed as described (47). Primers used for probe amplification are listed in Table S1.

Transient Expression Regulation Assays in *N. benthamiana* Leaves. The transient expression assays were performed in *N. benthamiana* leaves as described (40). The relevant PCR primer sequences are given in Table S1.

EMSA. EMSA was performed by using a LightShift Chemiluminescent EMSA kit (Thermo Scientific). The probe sequences of *OsCKX2* are listed in Table S2.

ChIP-PCR Assay. ChIP-PCR was carried out as described (40). Primers used for ChIP-PCR are listed in Table S1.

Accession Codes. Genes, and their associated accession codes from GenBank are as follows: *DST* (GQ178286.1); *OsRR1* (AB249661.1); *OsCKX2* (NM_001048837.1); *OsCKX1* (NM_001048787.1); *OsCKX3* (NM_001071421.1); *OsCKX4* (NM_001051888.1); *OsCKX9* (NM_001061906.2); *OsCKX11* (NM_001068512.1); *OsACT1* (NM_001057621.1); and *NbACT1* (EU938079.1).

Genes, and their associated accession codes from Rice Annotation Project Database are as follows: *OsCKX7* (LOC_Os02g12780.1); *OsCKX8* (LOC_Os04g44230.1); and *OsCKX10* (LOC_Os06g37500.1).

ACKNOWLEDGMENTS. We thank Y. Xue for critical comments and advice, J. Li for providing the pTCK303/1460 vector, C. Gao for generating transgenic wheat plants, and Z. Yuan and W. Luo for taking care of the rice plants. This work was supported by the National Natural Science Foundation of China Grants 90717007 and 91117013.

1. Sakamoto T, Matsuoka M (2004) Generating high-yielding varieties by genetic manipulation of plant architecture. *Curr Opin Biotechnol* 15(2):144–147.
2. Wang Y, Li J (2008) Rice, rising. *Nat Genet* 40(11):1273–1275.
3. Sakamoto T, Matsuoka M (2008) Identifying and exploiting grain yield genes in rice. *Curr Opin Plant Biol* 11(2):209–214.
4. Komatsu K, et al. (2003) LAX and SPA: Major regulators of shoot branching in rice. *Proc Natl Acad Sci USA* 100(20):11765–11770.
5. Ikeda K, Ito M, Nagasawa N, Kyozuka J, Nagato Y (2007) Rice ABERRANT PANICLE ORGANIZATION 1, encoding an F-box protein, regulates meristem fate. *Plant J* 51(6):1030–1040.
6. Kurakawa T, et al. (2007) Direct control of shoot meristem activity by a cytokinin-activating enzyme. *Nature* 445(7128):652–655.
7. Ashikari M, et al. (2005) Cytokinin oxidase regulates rice grain production. *Science* 309(5735):741–745.
8. Tan L, et al. (2008) Control of a key transition from prostrate to erect growth in rice domestication. *Nat Genet* 40(11):1360–1364.
9. Jin J, et al. (2008) Genetic control of rice plant architecture under domestication. *Nat Genet* 40(11):1365–1369.
10. Huang X, et al. (2009) Natural variation at the DEP1 locus enhances grain yield in rice. *Nat Genet* 41(4):494–497.
11. Miura K, et al. (2010) OsSPL14 promotes panicle branching and higher grain productivity in rice. *Nat Genet* 42(6):545–549.
12. Jiao Y, et al. (2010) Regulation of OsSPL14 by OsmiR156 defines ideal plant architecture in rice. *Nat Genet* 42(6):541–544.
13. Ikeda-Kawakatsu K, et al. (2009) Expression level of ABERRANT PANICLE ORGANIZATION1 determines rice inflorescence form through control of cell proliferation in the meristem. *Plant Physiol* 150(2):736–747.
14. Ookawa T, et al. (2010) New approach for rice improvement using a pleiotropic QTL gene for lodging resistance and yield. *Nat Commun* 1:132.
15. Tucker MR, Laux T (2007) Connecting the paths in plant stem cell regulation. *Trends Cell Biol* 17(8):403–410.
16. Veit B (2009) Hormone mediated regulation of the shoot apical meristem. *Plant Mol Biol* 69(4):397–408.
17. Werner T, Motyka V, Strnad M, Schmülling T (2001) Regulation of plant growth by cytokinin. *Proc Natl Acad Sci USA* 98(18):10487–10492.
18. Werner T, et al. (2003) Cytokinin-deficient transgenic Arabidopsis plants show multiple developmental alterations indicating opposite functions of cytokinins in the regulation of shoot and root meristem activity. *Plant Cell* 15(11):2532–2550.
19. Higuchi M, et al. (2004) In planta functions of the Arabidopsis cytokinin receptor family. *Proc Natl Acad Sci USA* 101(23):8821–8826.
20. Nishimura C, et al. (2004) Histidine kinase homologs that act as cytokinin receptors possess overlapping functions in the regulation of shoot and root growth in *Arabidopsis*. *Plant Cell* 16(6):1365–1377.
21. Riefler M, Novak O, Strnad M, Schmülling T (2006) Arabidopsis cytokinin receptor mutants reveal functions in shoot growth, leaf senescence, seed size, germination, root development, and cytokinin metabolism. *Plant Cell* 18(1):40–54.
22. Heyl A, et al. (2008) The transcriptional repressor ARR1-SRDX suppresses pleiotropic cytokinin activities in Arabidopsis. *Plant Physiol* 147(3):1380–1395.
23. Chaudhury AM, Letham S, Craig S, Dennis ES (1993) amp1-a mutant with high cytokinin levels and altered embryonic pattern, faster vegetative growth, constitutive photomorphogenesis and precocious flowering. *Plant J* 4:907–916.
24. Rupp HM, Frank M, Werner T, Strnad M, Schmülling T (1999) Increased steady state mRNA levels of the STM and KNAT1 homeobox genes in cytokinin overproducing Arabidopsis thaliana indicate a role for cytokinins in the shoot apical meristem. *Plant J* 18(5):557–563.
25. Bartrina I, Otto E, Strnad M, Werner T, Schmülling T (2011) Cytokinin regulates the activity of reproductive meristems, flower organ size, ovule formation, and thus seed yield in Arabidopsis thaliana. *Plant Cell* 23(1):69–80.
26. Werner T, Köllmer I, Bartrina I, Holst K, Schmülling T (2006) New insights into the biology of cytokinin degradation. *Plant Biol (Stuttg)* 8(3):371–381.
27. Huang XY, et al. (2009) A previously unknown zinc finger protein, DST, regulates drought and salt tolerance in rice via stomatal aperture control. *Genes Dev* 23(15):1805–1817.
28. Kuroha T, et al. (2009) Functional analyses of LONELY GUY cytokinin-activating enzymes reveal the importance of the direct activation pathway in Arabidopsis. *Plant Cell* 21(10):3152–3169.
29. Jain M, Tyagi AK, Khurana JP (2006) Molecular characterization and differential expression of cytokinin-responsive type-A response regulators in rice (Oryza sativa). *BMC Plant Biol* 6:1.
30. Ohta M, Matsui K, Hiratsu K, Shinshi H, Ohme-Takagi M (2001) Repression domains of class II ERF transcriptional repressors share an essential motif for active repression. *Plant Cell* 13(8):1959–1968.
31. Hiratsu K, Ohta M, Matsui K, Ohme-Takagi M (2002) The SUPERMAN protein is an active repressor whose carboxy-terminal repression domain is required for the development of normal flowers. *FEBS Lett* 514(2-3):351–354.
32. Tiwari SB, Hagen G, Guilfoyle TJ (2004) Aux/IAA proteins contain a potent transcriptional repression domain. *Plant Cell* 16(2):533–543.
33. Tsukagoshi H, Saijo T, Shibata D, Morikami A, Nakamura K (2005) Analysis of a sugar response mutant of Arabidopsis identified a novel B3 domain protein that functions as an active transcriptional repressor. *Plant Physiol* 138(2):675–685.
34. Kagale S, Links MG, Rozwadowski K (2010) Genome-wide analysis of ethylene-responsive element binding factor-associated amphiphilic repression motif-containing transcriptional regulators in Arabidopsis. *Plant Physiol* 152(3):1109–1134.
35. Weigel RR, Pfitzner UM, Gatz C (2005) Interaction of NIMIN1 with NPR1 modulates PR gene expression in Arabidopsis. *Plant Cell* 17(4):1279–1291.
36. Pauwels L, et al. (2010) NINJA connects the co-repressor TOPLESS to jasmonate signalling. *Nature* 464(7289):788–791.
37. Kim SH, et al. (2004) CAZFP1, Cys2/His2-type zinc-finger transcription factor gene functions as a pathogen-induced early-defense gene in Capsicum annuum. *Plant Mol Biol* 55(6):883–904.
38. Shang Y, et al. (2010) The Mg-chelatase H subunit of Arabidopsis antagonizes a group of WRKY transcription repressors to relieve ABA-responsive genes of inhibition. *Plant Cell* 22(6):1909–1935.
39. Qi T, et al. (2011) The Jasmonate-ZIM-domain proteins interact with the WD-Repeat/bHLH/MYB complexes to regulate Jasmonate-mediated anthocyanin accumulation and trichome initiation in Arabidopsis thaliana. *Plant Cell* 23(5):1795–1814.
40. Chen Q, et al. (2011) The basic helix-loop-helix transcription factor MYC2 directly represses PLETHORA expression during jasmonate-mediated modulation of the root stem cell niche in Arabidopsis. *Plant Cell* 23(9):3335–3352.
41. Yu J, et al. (2002) A draft sequence of the rice genome (Oryza sativa L. ssp. indica). *Science* 296(5565):79–92.
42. Shani E, Yanai O, Ori N (2006) The role of hormones in shoot apical meristem function. *Curr Opin Plant Biol* 9(5):484–489.
43. Jasinski S, et al. (2005) KNOX action in Arabidopsis is mediated by coordinate regulation of cytokinin and gibberellin activities. *Curr Biol* 15(17):1560–1565.
44. Leibfried A, et al. (2005) WUSCHEL controls meristem function by direct regulation of cytokinin-inducible response regulators. *Nature* 438(7071):1172–1175.
45. Yanai O, et al. (2005) Arabidopsis KNOXI proteins activate cytokinin biosynthesis. *Curr Biol* 15(17):1566–1571.
46. Liu Z, Wei F, Feng YQ (2010) Determination of cytokinins in plant samples by polymer monolith microextraction coupled with hydrophilic interaction chromatography-tandem mass spectrometry. *Anal Methods* 2:1676–1685.
47. Qi J, et al. (2008) Mutation of the rice Narrow leaf1 gene, which encodes a novel protein, affects vein patterning and polar auxin transport. *Plant Physiol* 147(4):1947–1959.